




Dark, photo and thermally driven conductivity of Ag-mixed $\text{Se}_{70}\text{Te}_{30}$ semiconducting thin films for thermoelectric applications

A. El-Denglawey¹, Pankaj Sharma^{2,*} , Pawan Kumar³, Ekta Sharma⁴, Dinesh C. Sati⁵, K. A. Aly^{6,7}, and A. Dahshan^{8,9}

¹Department of Physics, College of University College at Turabah, Taif University, PO Box 11099, Taif 21944, Saudi Arabia

²Applied Science Department, National Institute of Technical Teachers Training and Research, Sector 26, Chandigarh 160019, India

³School of Physics & Materials Science, Shoolini University, Solan, India

⁴Department of Physics and Materials Science, Jaypee University of Information Technology, Wagnaghat, Solan, H.P. 173234, India

⁵Government Post Graduate College, Gopeshwar, Chamoli, Uttarakhand 246401, India

⁶Department of Physics, Faculty of Science, Al-Azhar University, Assiut Branch, Assiut, Egypt

⁷Department of Physics, Faculty of Science and Arts, Jeddah University, Jeddah, Saudi Arabia

⁸Department of Physics, Faculty of Science, King Khalid University, P.O. Box 9004, Abha, Saudi Arabia

⁹Department of Physics, Faculty of Science, Port Said University, Port Said, Egypt

Received: 27 May 2021

Accepted: 28 August 2021

Published online:

19 September 2021

© The Author(s), under exclusive licence to Springer Science+Business Media, LLC, part of Springer Nature 2021

ABSTRACT

The Ag-mixed $\text{Se}_{70}\text{Te}_{30}$ thermally deposited semiconducting thin films show interesting thermoelectric properties. As the Ag content in the structure of $\text{Se}_{70}\text{Te}_{30}$ increases, the Seebeck coefficient increases. The semiconductive thin films reveal a *p*-type behavior. The dark conductivity increases at 300 K, whereas a reduction in corresponding activation energy for dark, photo and thermal response is observed with the increase in the Ag content. It is elucidated that the power factor for $(\text{Se}_{70}\text{Te}_{30})_{100-x}\text{Ag}_x$ ($0.0 \leq x \leq 8.0$ at.%) semiconducting thin films can be tuned and enhanced at varied temperature ranges through adjusting the addition amount of Ag. These results indicate that these semiconducting thin films have remarkable potential as thermoelectric generators.

1 Introduction

In recent years, the rapid increase in the consumption of fossil fuels has affected the global environment. As a result, there is increasing concern about devising effective solar heat/energy conversion methods into sustainable and renewable energy. Many researchers

develop waste heat recovery tools that require waste heat accumulation and its reuse in industrial heating processes or related mechanical and electrical projects [1–3]. The most advanced methods to transforming solar and/or waste heat into electrical energy are advanced thermoelectrics and vice versa [4–6]. Several phenomena are there in the solids

Address correspondence to E-mail: pks_phy@yahoo.co.in

regarding thermoelectricity, and these phenomena relate to the exchange of energy and transport between electrons and phonons. Current studies indicate that the best solution for heat recovery from waste is the thermoelectric generator which employs the Seebeck effect principle [7–9]. Commercialization on a large scale is still limited for thermoelectric generators owing to their performance components viz. thermoelectric figure-of-merit $zT = S^2\sigma T/\kappa = S^2\sigma T/(\kappa_l + \kappa_e)$, where κ , κ_l , κ_e , T , σ , and S denote the thermal conductivity, lattice thermal conductivity, electronic thermal conductivity, absolute temperature, electrical conductivity, and Seebeck coefficient, respectively [10]. To obtain high zT thermoelectric materials, compatibility of high-power factor ($S\sigma$) and low thermal conductivity ($\kappa_l + \kappa_e$) is required, but because of the combined nature of these parameters, it is rather a problem to fine-tune the zT parameter. A number of methods are explored to enhance the zT parameter, which includes tuning the bandgap through composition to optimize the power factor, controlling the carrier concentration, and nanostructure engineering to reduce the lattice thermal conductivity κ_l [11–15].

Chalcogenides typically show semiconducting properties. They are relevant candidates for technological applications like sensors, optoelectronics, solar cells, and thermoelectrics [16–18]. Conventional thermoelectric materials with high zT are constituted by heavily doped small bandgap semiconductors or semimetals, among these chalcogenides (S-, Se-, Te-based compounds), particularly Te-based are the most investigated [19–21]. Among chalcogens (S, Se, Te), Te is more metallic and crystallizes easily than S and Se, and hence has high electrical conductivity along with high thermal conductivity [19–21]. To reduce the thermal conductivity and structural disorder can be introduced by making the system glassier or reducing crystallinity. Therefore, for a system to have high zT it must have a small thermal conductivity, a large Seebeck coefficient, and a large electrical conductivity [8, 9]. In this report, we have considered Se–Te chalcogenide glass as a starting material with Se 70 at.% and Te 30 at.%, this composition is supposed to take care of the low thermal conductivity as Se is a very good glass former, but simultaneously it also reduced the electronic conductivity [8]. For the high-power factor ($S\sigma$) requirement, the electronic conductivity needs to be improved, and here silver (Ag) is introduced into the

system. Particularly, in chalcogenide glasses Ag increases the concentration of the charge carrier, ensuing in an enhancement of the electrical conductivity.

This article explores the effect of incorporating Ag on the dark conductivity, photoconductivity, and Seebeck coefficient, along with the thorough understanding of free carrier lifetime, spectral distribution of photocurrent and carrier concentrations for the vacuum evaporated $(\text{Se}_{70}\text{Te}_{30})_{100-x}\text{Ag}_x$ ($0.0 \leq x \leq 8.0$ at.%) thin films.

2 Experimental details

Thermal evaporation technique has been employed to deposit the thin films of melt quenched $(\text{Se}_{70}\text{Te}_{30})_{100-x}\text{Ag}_x$ ($0.0 \leq x \leq 8.0$ at.%) glassy system in a vacuum coating unit, Edward 306A, in a high vacuum of 10^{-5} mbar at room temperature. Microscopic glass slides are used as substrates. Electrodes of Au are deposited on the thin films at a spacing of 1 mm and length of ~ 1.4 mm using DC sputtering Desk V (Denton Vacuum) for the dark- and photo-electrical measurements. For the study of thermoelectric power, the length and spacing of Au electrodes are 1.4 mm and 1 mm, respectively. For the dark- and photo-electrical measurements, the measuring system contains a regulator Pasco, model 1030A dc power supply with the specimen and 6517B Keithley electrometer. Monochromatic light has been achieved using MQ3-Zeiss monochromator. A 200 W power tungsten lamp was used. The photocurrent (I_{ph}) was taken as the difference among the currents with and without lighting.

The 2-probe method is employed. For thermoelectric power measurements, a temperature difference ($T_2 - T_1$) of 15 °C is maintained between the two extreme ends of the thin film sample. To monitor the temperatures T_1 and T_2 of the two extreme ends of the thin film sample, two copper–constantan thermocouples are fixed with a thermally conductive silicon paste. The average of T_1 and T_2 is taken as the sample temperature. Dark conductivity and thermoelectric power are performed within the temperature range 300–420 K under $\approx 10^{-3}$ Torr vacuum. The energy dispersive X-ray spectroscopy (EDX) and X-ray diffraction (XRD) instrumentation and other parameters for the investigated compositions may be seen elsewhere [22].

3 Results and discussion

Figure 1 demonstrates the amorphous nature of the as-deposited thin films as XRD patterns show no prominent peak [22]. Compositional analysis for the as-deposited thin films has been conducted using EDX, and the results are in good conformity with the initial compositions (Table 1) [22]. The morphology of the thin films is investigated employing scanning electron microscope is shown in Fig. 2. Usually, amorphous material/thin film does not show any remarkable features in SEM images, however, Ag incorporated chalcogenides composition claimed to have some phase segregation [23, 24]. But, in the studied composition SEM images do not indicate any Ag clustering. So, it is believed further surface morphological studies will be not so informative.

Figure 3 shows the temperature dependence of the dark electrical conductivity (σ_d) for $(\text{Se}_{70}\text{Te}_{30})_{100-x}\text{Ag}_x$ ($0.0 \leq x \leq 8.0$ at.%) thin films with increasing Ag content. Further, it can be seen Ag content strongly affects the σ_d as is envisaged from Fig. 3. The plots obtained in Fig. 3 are straight lines for all the investigated samples, confirming that the electrical conduction originates through an activated process.

It can be seen that with increasing the temperature the dark conductivity strongly increases, and hence there is single activation energy in the temperature range 300–420 K. Therefore, in the investigated

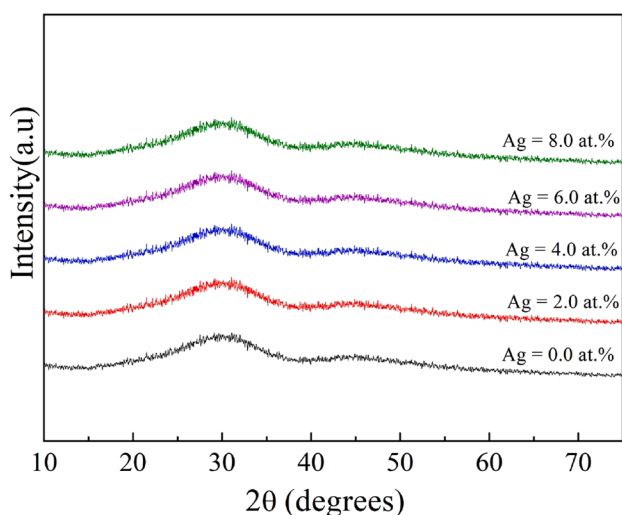


Fig. 1 XRD patterns for $(\text{Se}_{70}\text{Te}_{30})_{100-x}\text{Ag}_x$ ($0.0 \leq x \leq 8.0$ at.%) films. Reprinted with permission from publication [22], Elsevier, License Number 5131770749192

Table 1 The EDX results for $(\text{Se}_{70}\text{Te}_{30})_{100-x}\text{Ag}_x$ ($0.0 \leq x \leq 8.0$ at.%) films. Reprinted with permission from publication [22], Elsevier, License Number 5131770749192

x at.%	Starting materials			As-prepared thin films		
	Se	Te	Ag	Se	Te	Ag
0	70	30	0	70.13	29.87	0
2	68.6	29.4	2	68.57	29.35	2.08
4	67.2	28.8	4	67.24	28.88	3.88
6	65.8	28.2	6	65.86	28.36	5.78
8	64.4	27.6	8	64.64	27.55	7.81

temperature range, the samples confirm an Arrhenius type behavior [25, 26];

$$\sigma_d = \sigma_o \exp\left(\frac{-\Delta E_d}{k_B T}\right), \quad (1)$$

where σ_o being a pre-factor, ΔE_d is the temperature-independent activation energy and k_B is the Boltzmann constant. An analysis, i.e. from slopes of the linear fits in Fig. 3 reveals that ΔE_d values decrease with increasing Ag content, while σ_o values are observed to increase. So, it is clear that both ΔE_d and σ_o values show dependency on the doping content (Table 2). A smaller value of σ_o points to an extensive range of localized states and conduction by hopping. The values of σ_o changed from 444 to 592 $\Omega^{-1} \text{m}^{-1}$ for $x = 0$ to $x = 8$, respectively. Therefore, it can be interpreted that the addition of Ag increases the density of localized states. Moreover, with the rise in Ag content in Se–Te system, the binding energy of the studied compositions reduces, possibly because of the lower bond energies of Ag–Se ($210 \pm 14.6 \text{ kJ mol}^{-1}$) and Ag–Ag ($162.9 \pm 2.9 \text{ kJ mol}^{-1}$) as opposed to Se–Te ($293.3 \text{ kJ mol}^{-1}$), Te–Te ($257.6 \pm 4.1 \text{ kJ mol}^{-1}$) and Se–Se ($330.5 \text{ kJ mol}^{-1}$) bonds [27]. This describes the σ_d increase at 300 K and the subsequent reduction in ΔE_d with the increase in the Ag content. Further, the increased ionic character of Ag–Se also accounts for the increase in conductivity.

Photoconductivity (σ_{ph}) plays a vital role in studying conduction mechanisms in chalcogenide materials [28–30]. The localization and delocalization of charge carriers are essential processes in the behavior of photocurrent. These mechanisms within the bandgap of glassy semiconductors are correlated with the localized states. The fundamental mechanisms that rule the generation of charge carriers on

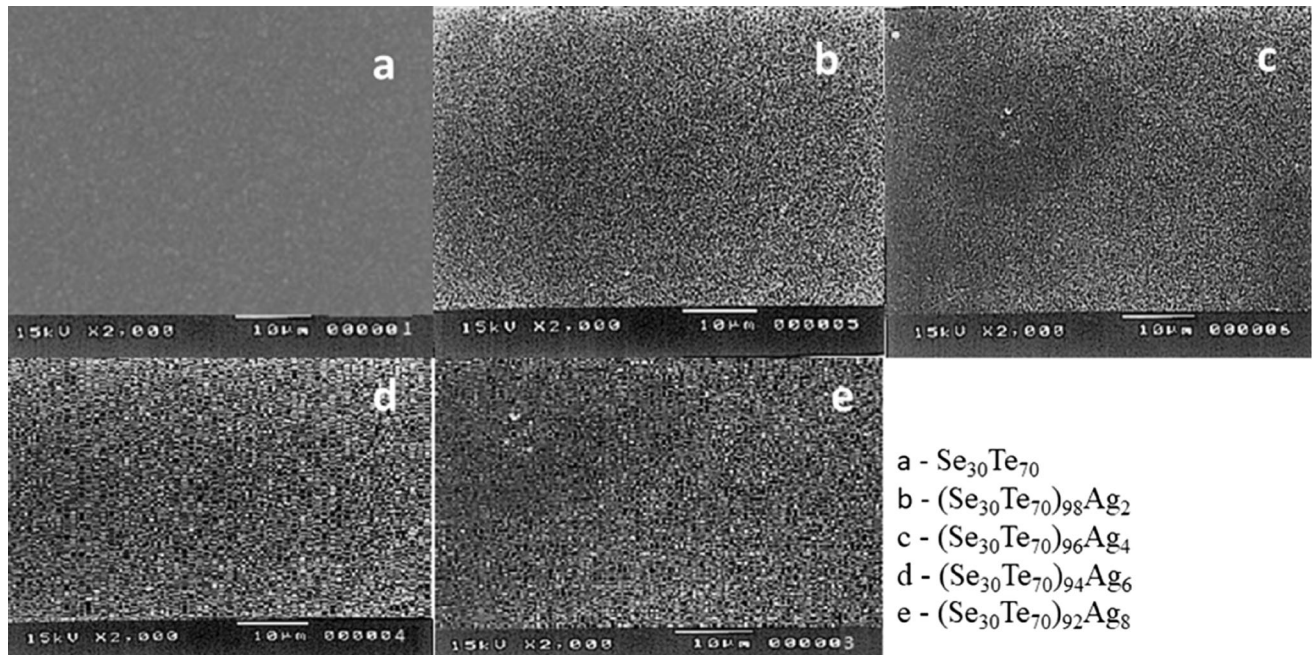


Fig. 2 a–e SEM micrographs of the as-deposited $(\text{Se}_{30}\text{Te}_{70})_{100-x}\text{Ag}_x$ films on a glass substrate

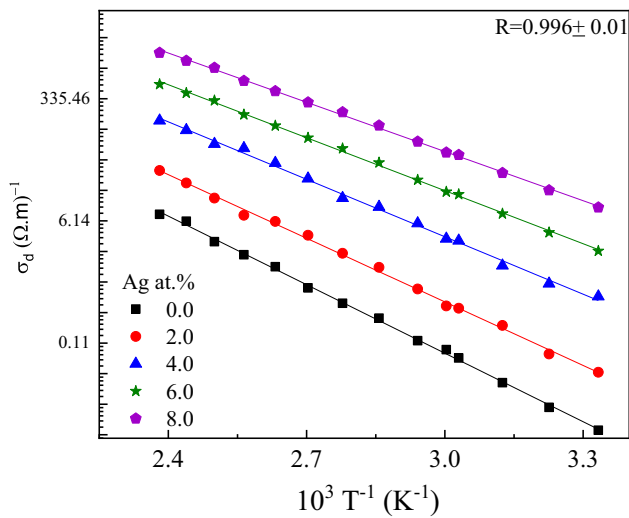


Fig. 3 Plots of σ_d versus $10^3/T$ for $(\text{Se}_{70}\text{Te}_{30})_{100-x}\text{Ag}_x$ ($0.0 \leq x \leq 8.0$ at.%) thin films

the absorption of incident photons, and their transport through the material on the application of an electric field, and their recombination. Measuring dc-photoconductivity (σ_{ph}) is an essential tool for understanding the kinetics of recombination of charged carriers.

Generally, the temperature-dependent of dc-photoconductivity in glassy semiconductors is threefold [31, 32].

- (i) At low temperatures, when the temperature changes σ_{ph} remains almost constant and changes linearly with light intensity, $\sigma_{ph} \propto G$ (G being the generation rate). This is because there is no phonon assistance for σ_{ph} .
- (ii) At the intermediate temperature region, where temperature rises by many orders of magnitude making σ_{ph} increase and it might be a characteristic of phonon assistance to charge carriers, and activation energy in this reign is correlated with the depth of the traps in the forbidden gap. Here, σ_{ph} is a sublinear function of current, and σ_d remains less than σ_{ph} . The rate of recombination remains regulated through the photogenerated charge carriers and $\sigma_{ph} \propto G^\gamma$.
- (iii) At high-temperature region, $\sigma_{ph} < \sigma_d$ since the number of photons excited thermally exceeds the number of light-driven carriers. Herewith an enhancement in temperature σ_{ph} decreases and stays proportional to I ($\sigma_{ph} \propto G$).

For $(\text{Se}_{70}\text{Te}_{30})_{100-x}\text{Ag}_x$ ($0.0 \leq x \leq 8.0$ at.%) thin films, at an applied electric field of $20,000 \text{ V m}^{-1}$, the photoconductivity is measured at room temperature 300 K (Fig. 4). The σ_{oph} values are observed to increase. From the slopes of plots in Fig. 4, the values of ΔE_{ph} are obtained and are found to decrease from

Table 2 Some electrical and thermoelectrical parameters for the $(\text{Se}_{70}\text{Te}_{30})_{100-x}\text{Ag}_x$ ($0.0 \leq x \leq 8.0$ at.%) thin films

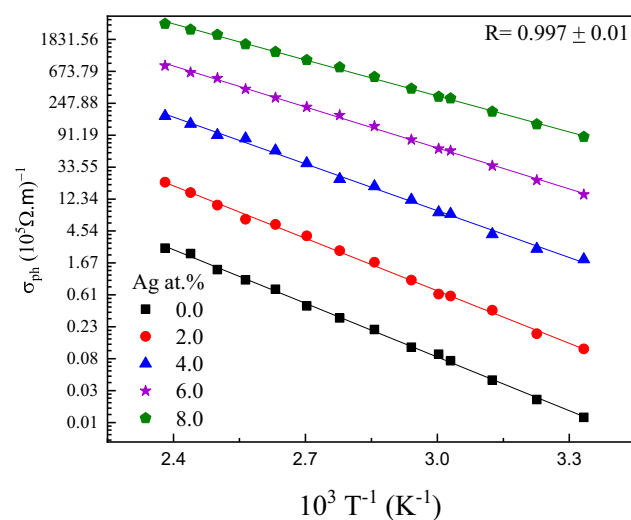
Ag (at.%)	σ_d^* $\times 10^{-8}$ $(\Omega \text{ m})^{-1}$	σ_{ph}^* $\times 10^{-5}$ $(\Omega \text{ m})^{-1}$	σ_o (Eq. 1)	σ_o (Eq. 4)	σ_{oph}	ΔE_d	ΔE_s	Δ	ΔE_{ph}	E_g	γ 10^{-3} eV K^{-1}	n_d 10^{15} m^{-3}	n_s 10^{17} m^{-3}	n_{ph} 10^{18} m^{-3}
0	0.65	0.01	444	446	17	0.65	0.55	0.091	0.48	1.3	6.371	0.37	0.33	0.37
2	4.32	0.11	475	478	96	0.60	0.52	0.081	0.47	1.19	6.391	2.29	1.38	2.29
4	51.8	1.87	535	536	200	0.54	0.47	0.073	0.42	1.08	6.458	24.28	12.7	24.28
6	230	14.2	563	563	230	0.50	0.44	0.058	0.37	0.99	6.612	102.5	46.9	102.5
8	955	86.6	592	590	247	0.46	0.42	0.044	0.32	0.91	6.738	404.9	109.6	404.9

0.48 to 0.32 eV (Table 2). So, it is clear that both ΔE_{ph} and σ_{oph} values show dependency on the doping content. Figure 4 shows that photoconductivity is an activated process. For photoconduction, the value of ΔE_{ph} also follows the same trend with the incorporation of Ag similar to ΔE_d for samples under investigation.

Using the pre-factors σ_o and σ_{oph} corresponding to dark and photoconductivity, respectively, the relaxation time of charge carrier in the dark (τ_d) or illuminated (τ_{ph}) conditions are determined under different temperatures employing the relation [33, 34];

$$\sigma_o = \frac{2e^2\tau}{m^*} \left(\frac{2\pi m^* k_B T}{h^2} \right)^{3/2} \quad (2)$$

m^* ($= 0.11 m_e$) is the charge carriers' effective mass [35], m_e denotes the mass of free electron and h symbolizes the Planck's constant. For the

**Fig. 4** Plot of σ_{ph} of $(\text{Se}_{70}\text{Te}_{30})_{100-x}\text{Ag}_x$ ($0.0 \leq x \leq 8.0$ at.%) thin films with $10^3/T$

$(\text{Se}_{70}\text{Te}_{30})_{100-x}\text{Ag}_x$ ($0.0 \leq x \leq 8.0$ at.%) thin films, the temperature dependence of relaxation time (τ) ($\tau = \tau_d$ for solid symbols, and $\tau = \tau_{ph}$ for hollow symbols) show an increase with Ag content (Fig. 5).

Photoconductive materials have spectral distribution curves with a more or less sharp peak near the absorption edge. Typically, the photoconductive response starts from zero and goes up quickly on reaching the absorption edge passes a maximum at a certain moderate absorption value and falls again as the absorption coefficient continues to increase and generally and usually seems to approach some non-zero asymptotic value. Figure 6 depicts the spectral distribution of dc-Photoconductivity for thin films under investigation at an applied electric field $20,000 \text{ V m}^{-1}$ and at ambient temperature. In the spectrum, it is observed that on replacing $\text{Se}_{70}\text{Te}_{30}$ with Ag content, the photocurrent peak shift to low wavelengths. These plots are employed to estimate the energy gap (E_g) values of $(\text{Se}_{70}\text{Te}_{30})_{100-x}\text{Ag}_x$ ($0.0 \leq x \leq 8.0$ at.%) thin films using the relation [36]; $E_g(\text{eV}) = hc/\lambda_{1/2}$, where $\lambda_{1/2}$ is the half-maximum wavelength corresponding to the peak photocurrent and c is the speed of light.

Figure 6 shows a decrease in photocurrent with increased Ag content and also the absorption peak shift to low energy indicating a decrease in E_g values (Table 2). This behavior is also supported by the optical bandgap estimated elsewhere using theoretical, and Tauc plot [22, 37]. This behavior can be explained with the help of the chemical bond approach [38].

The most advanced methods to transforming solar and/or waste heat into electrical energy are advanced thermoelectrics. A number of phenomena are there in the solids in respect of thermoelectricity, and these phenomena relate to the exchange of

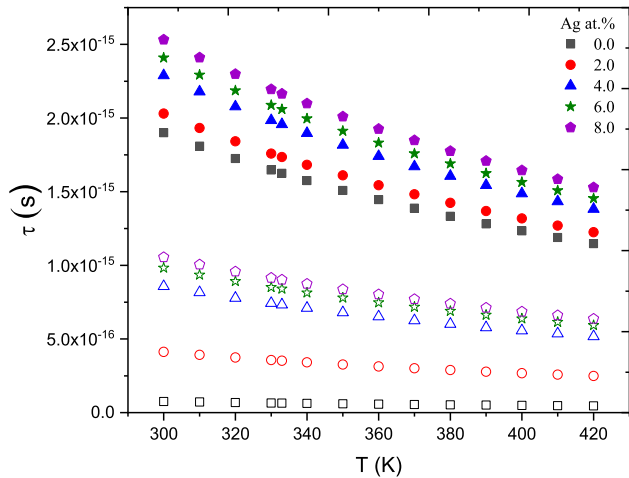


Fig. 5 The temperature dependence of relaxation time (τ) ($\tau = \tau_d$ for solid symbols, and ($\tau = \tau_{ph}$ for hollow symbols) of $(\text{Se}_{70}\text{Te}_{30})_{100-x}\text{Ag}_x$ ($0.0 \leq x \leq 8.0$ at.%) thin films

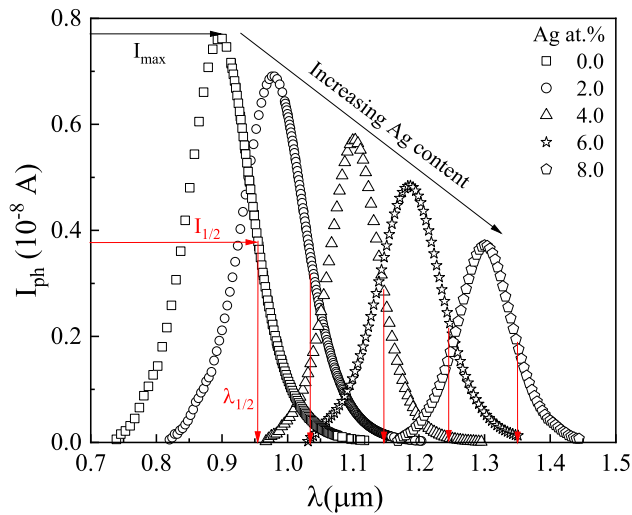


Fig. 6 dc-photocurrent spectral distribution of $(\text{Se}_{70}\text{Te}_{30})_{100-x}\text{Ag}_x$ ($0.0 \leq x \leq 8.0$ at.%) thin films

energy and transport between electrons and phonons. The best solution for heat recovery from waste is the thermoelectric generator which employs the Seebeck effect principle. Commercialization on a large scale is still limited for thermoelectric generators owing to their performance components viz. thermoelectric figure-of-merit $zT = S^2\sigma T / (\kappa_l + \kappa_e)$, where κ , κ_l , κ_e , T , σ , and S denote the thermal conductivity, lattice thermal conductivity and electronic thermal conductivity, absolute temperature, electrical conductivity, and Seebeck coefficient, respectively.

In order to have the appropriate thermoelectric power or Seebeck coefficient (S) and electrical

conductivity, the performance of thermoelectric material is governed by the appropriate electronic band structure. The thermoelectric power exhibits the intrinsic band structure. Control of concentration of the charge carriers may permit the value of S to be tuned in a certain range. This is why the search for novel thermoelectric materials involves both electric conductivity and thermoelectric power measurements. Thermoelectric power (S), in the presence of a temperature gradient, is not only an induced voltage but also contains precious evidence about the description of the glass semiconductors. Actually, the parameter S renders the extra information about the type of charge carriers along with their concentration [39, 40]. The magnitude of the Seebeck coefficient is computed from the energy dependence of the carrier relaxation time, the density of states and the Fermi level. Seebeck coefficient has been discussed for amorphous semiconductors in [39, 40]. Here it is important to remember that the values of S depend on the density of states and the Fermi level. It is especially experimentally found that a large number of states above the Fermi level can obtain a large S value. The S coefficient for a non-degenerate semiconductor of p -type is represented as follows [25, 41];

$$S = \frac{k}{e} \left(\frac{\Delta E_S}{KT} + A \right) = \frac{k}{e} \left(\frac{E_f - E_v}{KT} + A \right) = \frac{k}{e} \left(\frac{E_0}{kT} - \frac{\gamma}{k} + A \right),$$

$$\frac{e}{k} S = \frac{E_0}{kT} - \frac{\gamma}{k} + A, \tag{3}$$

where A is a constant (assumed unity for n -semiconductors) related to the carrier scattering mechanism, E_v represents the top of the valence band energy and E_f denotes Fermi energy. In Eq. (3), it is supposed that the energy splitting $\Delta E_S = E_f - E_v$ varies linearly with temperature as $E_f - E_v = E_0 - \gamma T$. Consequently, from Fig. 7, γ and E_0 are assessed from the intercept and the slope of S , respectively. So, when $\Delta E_S < \Delta E_d$, the difference $\Delta^* = \Delta E_d - \Delta E_S$ is the barrier of polaron-hopping [42]. This is called the conduction mechanism of small polarons. Here, the presence of Se in the glass network is linked to this effect [43]. For $(\text{Se}_{70}\text{Te}_{30})_{100-x}\text{Ag}_x$ ($0.0 \leq x \leq 8.0$ at.%) thin films, the variation of S with temperature reveals large positive values as depicted in Fig. 7. This indicates that the samples under investigation are of p -type. The absolute value of the Seebeck coefficient (S) of Ag mixed Se–Te declines. This is on account of the increase of free charge carrier concentrations

(calculated later). The values of ΔE_S and Δ show a decrease with increasing Ag content (Table 2). Suppose one can look at the increase in the conductivity values (calculated later) and the S values. In that case, the product increases the power factor ($P = S\sigma$), making these compositions a better perspective for thermoelectric applications.

For p -type semiconductors, conductivity can also be correlated with the Seebeck coefficient through the relation [25]; $\sigma_d = \sigma_o \exp\left(\frac{-(E_F - E_v)}{kT}\right) = \sigma_o \exp\left(\frac{e}{k}\right) \exp\left(\frac{-E_o}{kT}\right)$, and combining this with Eq. (3) the relation becomes;

$$\ln(\sigma_d) = \frac{-e}{k} S + (\ln(\sigma_o) + A) \quad (4)$$

Figure 8 shows the variation of $\ln(\sigma_d)$ with Seebeck coefficient give straight lines whose slope give the value of (e/k) and the intercept give the value of $(\ln(\sigma_o) + A)$. The values slope and in good agreement with the theoretical value of (e/k) , and the value of σ_o obtained show an increase with the increase of Ag content in Se–Te system (Table 2).

Figure 9 shows free charge carrier concentration obtained from (a) dark conductivity (n_d) (b) obtained from photoconductivity n_{ph} , and (c) obtained from Seebeck coefficient n_s with temperature for $(\text{Se}_{70}\text{Te}_{30})_{100-x}\text{Ag}_x$ ($0.0 \leq x \leq 8.0$ at.%) thin films employing respective the relations [25, 44];

$$n_d = 2M^{3/2} \exp\left(\frac{-\Delta E_d}{k_B T}\right) \quad (5a)$$

$$n_{ph} = 2M^{3/2} \exp\left(\frac{-\Delta E_{ph}}{k_B T}\right) \quad (5b)$$

$$n_s = \frac{\pi}{3} \left(\frac{8\pi^2 k_B^2 m^* T}{3Seh^2}\right)^{3/2}, \quad (5c)$$

where $M = 2\pi m^* k_B T / h^2$. The values of n_d , n_{ph} , and n_s show an increase with the Ag content, whereas for a particular composition, $n_{ph} > n_s > n_d$ (Table 2). So, it is observed that the product of coefficient S and conductivity σ i.e. power factor increases with the enhancement of Ag content in Se–Te system. It is elucidated that the power factor for $(\text{Se}_{70}\text{Te}_{30})_{100-x}\text{Ag}_x$ ($0.0 \leq x \leq 8.0$ at.%) semiconducting thin films can be tuned and enhanced at varied temperature ranges through changing the adding amount of Ag.

4 Conclusions

$(\text{Se}_{70}\text{Te}_{30})_{100-x}\text{Ag}_x$ ($0.0 \leq x \leq 8.0$ at.%) semiconducting thin films deposited employing thermal evaporation have been analyzed for the dark- and photoconductivities. Seebeck coefficient and conductivities have been computed, and it is observed that the power factor shows an enhancement with the addition of Ag content. The free charge carriers concentration has also been obtained from dark conductivity,

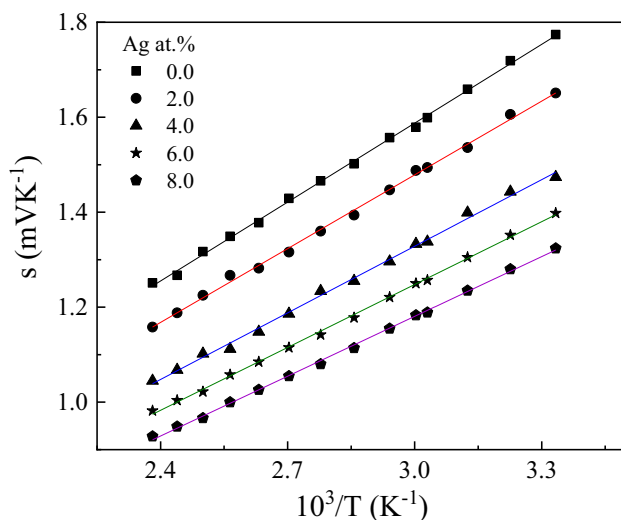


Fig. 7 Graphs of Seebeck coefficient S versus $10^3/T$ of $(\text{Se}_{70}\text{Te}_{30})_{100-x}\text{Ag}_x$ ($0.0 \leq x \leq 8.0$ at.%) thin films

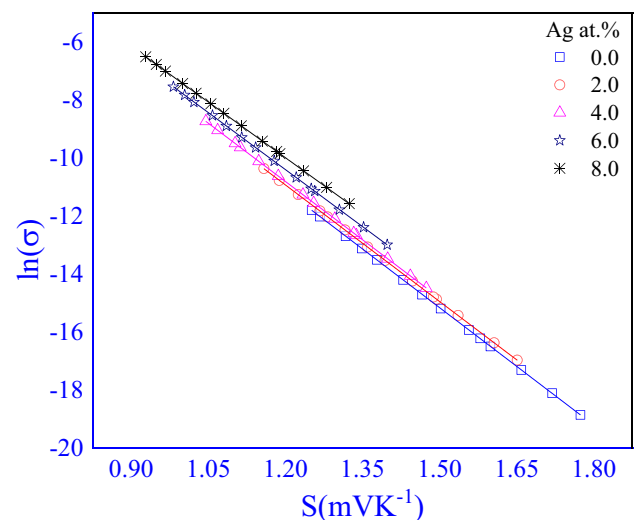


Fig. 8 Plots of $\ln(\sigma_d)$ versus S of $(\text{Se}_{70}\text{Te}_{30})_{100-x}\text{Ag}_x$ ($0.0 \leq x \leq 8.0$ at.%) thin films

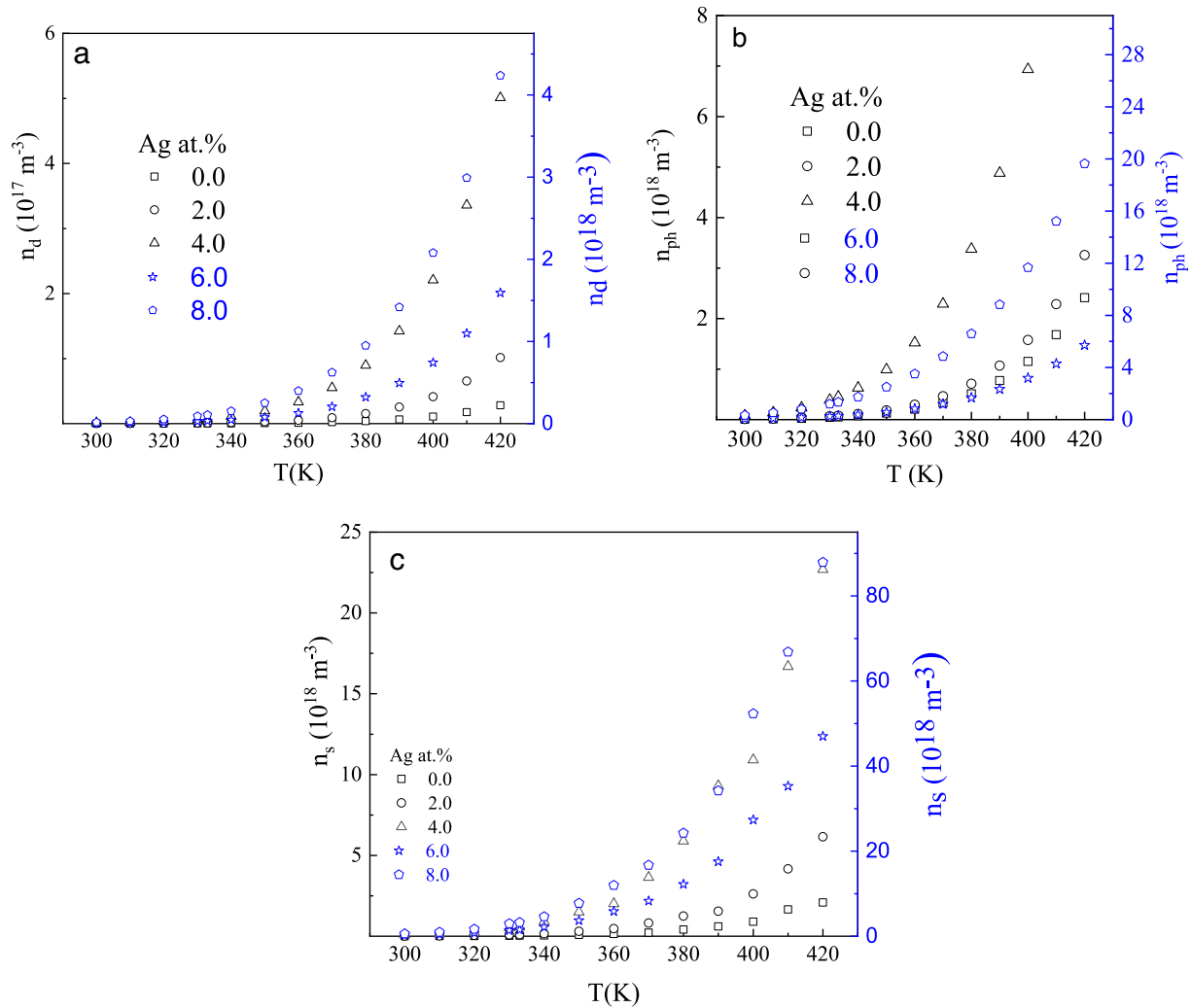


Fig. 9 Variations of charge carrier concentration **a** n_d obtained from dark conductivity, **b** n_{ph} obtained from photoconductivity and **c** n_s obtained from Seebeck coefficient with temperature for

$(Se_{70}Te_{30})_{100-x}Ag_x$ ($0.0 \leq x \leq 8.0$ at.%) thin films (Note For $x = 0, 2, 4$ read the y -axis on left side, and for $x = 6, 8$ read the y -axis on right side)

photoconductivity, and Seebeck coefficient, and found that for a particular composition, $n_{ph} > n_s > n_d$. The power factor for $(Se_{70}Te_{30})_{100-x}Ag_x$ ($0.0 \leq x \leq 8.0$ at.%) semiconducting thin films can be tuned and enhanced at varied temperature ranges by adjusting the addition amount of Ag. These findings reveal the remarkable ability of these thin semiconducting films for thermoelectric applications.

Acknowledgements

The author (A El-Denglawey) grateful to Taif University Researchers Supporting Project Number

(TURSP-2020/45) Taif University, Taif, Saudi Arabia. The author (A. Dahshan) extends his appreciation to the Deanship of Scientific Research at King Khalid University for funding this work through research groups program under Grant Number (RGP.2/89/42).

Funding

Funding was provided by Taif University (Grant No. TURSP-2020/45) and King Khalid University (Grant No. RGP.2/89/42).

Declarations

Conflict of interest The authors declare that they have no known competing financial interests or personal relationships that could have appeared to influence the work reported in this paper.

References

- Z.G. Chen, X.L. Shi, L.D. Zhao, J. Zou, *Prog. Mater. Sci.* **97**, 283–346 (2018)
- M.S. Dresselhaus, G. Chen, M.Y. Tang, R.G. Yang, H. Lee, D.Z. Wang, Z.F. Ren, J.P. Fleurial, P. Gogna, *Adv. Mater.* **19**, 1043–1053 (2007)
- Y. Xiao, L.D. Zhao, *Science* **367**, 1196–1197 (2020)
- A.M. Adam, E.M.M. Ibrahim, A. Panbude, K. Jayabal, P. Veluswamy, A.K. Diab, *J. Alloys Compd.* **872**, 159630 (2021)
- F.J. DiSalvo, Thermoelectric cooling and power generation. *Science* **285**, 703 (1999)
- L.E. Bell, *Science* **321**, 1457 (2008)
- L. Yang, Z.G. Chen, M.S. Dargusch, J. Zou, *Adv. Energy Mater.* **8**, 1701797 (2018)
- P. Sharma, A. Dahshan, V.K. Sehgal, K.A. Aly, *IEEE Trans. Electron Devices* **65**(8), 3408–3413 (2018)
- A. Dahshan, H.H. Hegazy, K.A. Aly, P. Sharma, *Physica B* **526**, 117–121 (2017)
- B. Yang, S. Li, X. Li, Z. Liu, H. Zhong, X. Li, S. Feng, *J. Alloys Compd.* **860**, 158245 (2021)
- K. Kaur, R. Kumar, *Prog. Nat. Sci. Mater. Int.* **26**(6), 533–539 (2016)
- Y. Wu, P. Nan, Z. Chen, Z. Zeng, R. Liu, H. Dong, L. Xie et al., *Adv. Sci.* **7**(12), 1902628 (2020)
- M. Murata, K. Nagase, K. Aoyama, A. Yamamoto, *Appl. Phys. Lett.* **117**(10), 103903 (2020)
- G. Hegde, A.N. Shridhar, A. Prabhu, Rao, M.K. Chattopadhyay, *Mater. Sci. Semicond. Process.* **127**, 105645 (2021)
- M.M. Alsalama, H. Hamoudi, A. Abdala, Z.K. Ghouri, K.M. Youssef, *Rev. Adv. Mater. Sci.* **59**(1), 371–378 (2020)
- P. Sharma, N. Sharma, S. Sharda, S.C. Katyal, V. Sharma, *Prog. Solid State Chem.* **44**(4), 131–141 (2016)
- S. Chand, N. Thakur, S.C. Katyal, P.B. Barman, V. Sharma, P. Sharma, *Sol. Energy Mater. Sol. Cells* **168**, 183–200 (2017)
- V. Sharma, S. Sharda, N. Sharma, S.C. Katyal, P. Sharma, *Prog. Solid State Chem.* **54**, 31–44 (2019)
- S. Lin, W. Li, Z. Chen, J. Shen, B. Ge, Y. Pei, *Nat. Commun.* **7**(1), 1–6 (2016)
- D.W. Newbrook, S.P. Richards, K. Victoria, V.K. Greenacre, A.L. Hector, W. Levason, G. Reid, C.H.K. de Groot, R. Huang, *ACS Appl. Energy Mater.* **3**(6), 5840–5846 (2020)
- Z. Gao, G. Liu, J. Ren, *ACS Appl. Mater. Interfaces* **10**(47), 40702–40709 (2018)
- A. El-Denglawey, V. Sharma, E. Sharma, K.A. Aly, A. Dahshan, P. Sharma, Optical and mechanical properties of Ag doped thermally evaporated SeTe thin films for optoelectronic applications. *J. Phys. Chem. Solids* **159**, 110291 (2021)
- S. Stehlik, J. Kolar, H. Haneda, I. Sakaguchi, M. Frumar, T. Wagner, Phase separation in chalcogenide glasses: the system AgAsS₂Se. *Int. J. Appl. Glass Sci.* **2**(4), 301–307 (2011)
- N. Mehta, A. Kumar, Observation of phase separation in some Se–Te–Ag chalcogenide glasses. *Mater. Chem. Phys.* **96**(1), 73–78 (2006)
- S. Znaidia, I. Kebaili, I. Boukhris, R. Neffati, H.H. Somaily, H. Algarni, H.H. Hegazy, K.A. Aly, A. Dahshan, *Appl. Phys. A* **126**(3), 1–8 (2020)
- I. Sharma, A. Kumar, S.K. Tripathi, P.B. Barman, *J. Phys. D Appl. Phys.* **41**(17), 175504 (2008)
- Y.-R. Luo, J.A. Kerr, *CRC Handb. Chem. Phys.* **89**, 89 (2012)
- S. Sharma, R. Sharma, P. Kumar, R. Thangaraj, K. Asokan, M. Mian, *J. Mater. Sci. Mater. Electron.* **28**(19), 14202–14208 (2017)
- O. Iaseniu, M. Iovu, *Rom. Rep. Phys.* **69**, 505 (2017)
- A. Kumar, R.K. Shukla, A. Kumar, R. Gupta, *Infrared Phys. Technol.* **102**, 103056 (2019)
- T.C. Arnoldussen, R.H. Bube, E.A. Fagen, S. Holmberg, *J. Appl. Phys.* **43**, 1798–1807 (1972)
- M. Di Giulio, G. Micocci, R. Rella, P. Siciliano, A. Tepore, *Thin Solid Films* **148**, 273–278 (1987)
- A. Dahshan, P. Sharma, K.A. Aly, *Dalton Trans.* **44**(33), 14799–14804 (2015)
- K.A. Aly, A. Dahshan, Gh. Abbady, Y. Saddeek, *Physica B* **497**, 1–5 (2016)
- Z.H. Khan, M. Zulfeqaur, A. Kumar, M. Husain, *Can. J. Phys.* **80**, 19–27 (2002)
- A. Dahshan, H.H. Amer, A.H. Moharam, A.A. Othman, *Thin Solid Films* **513**(1–2), 369–373 (2006)
- A. El-Denglawey, K.A. Aly, E. Sharma, R. Arora, S. Sharda, P. Sharma, A. Dahshan, Topological analysis and glass kinetics of Se-Te-Ag lone pair semiconductors. *Phys. Scr.* (2021). <https://doi.org/10.1088/1402-4896/ac2709>
- J. Bicerano, S.R. Ovshinsky, *J. Non-Cryst. Solids* **74**(1), 75–84 (1985)
- J. Martin, L. Wang, L. Chen, G.S. Nolas, *Phys. Rev. B* **79**(11), 115311 (2009)
- H. Fritzsche, *Solid State Commun.* **9**, 1813 (1971)
- H. Fritzsche, in *Amorphous and Liquid Semiconductors*. ed. by J. Tauc (Plenum Press, New York, 1971)

42. D. Emin, *Philos. Mag.* **99**(10), 1225–1239 (2019)
43. D. Emin, C.H. Seager, R.K. Quinn, *Phys. Rev. Lett.* **28**(13), 813–816 (1972)
44. S. Shukla, S.P. Singh, S. Kumar, *Indian J. Pure Appl. Phys.* **49**, 545–549 (2011)

Publisher's Note Springer Nature remains neutral with regard to jurisdictional claims in published maps and institutional affiliations.